

ABOUT COMPETITION BETWEEN TETRAHEDRAL AND OCTAHEDRAL SYMMETRIES IN ATOMIC NUCLEI*

I. DEDES^a, J. DUDEK^{a,b}, J. YANG^a, A. BARAN^a, D. CURIEN^b
H.L. WANG^{b,c}

^aInstitute of Physics, Maria Curie-Skłodowska University
pl. Marii Curie-Skłodowskiej 1, 20-031 Lublin, Poland

^bUniversité de Strasbourg, IPHC
23, rue du Loess, 67037 Strasbourg, France
and

CNRS, UMR7178, 67037 Strasbourg, France

^cSchool of Physics and Engineering, Zhengzhou University
Zhengzhou 450001, China

(Received December 21, 2018)

Following a recent discovery of the simultaneous signs of the octahedral and tetrahedral symmetries in ^{152}Sm , we discuss the issue of a competition between the two symmetries in atomic nuclei together with the identification criteria. Illustrations using selected rare-earth and zirconium nuclei as examples are presented.

DOI:10.5506/APhysPolBSupp.12.557

1. Introduction

The issue of finding an evidence of the presence of tetrahedral symmetry in atomic nuclei preoccupied several authors in the past, both theorists and experimentalists. Among the first theory predictions obtained with the help of a realistic phenomenological mean-field approach, which indicated the presence of the well-pronounced tetrahedral (T_d) symmetry minima in some heavy even–even nuclei, are those of Ref. [1]. The authors pointed out the existence of the new spectroscopic properties of the single-particle spectra of the mean-field Hamiltonians with tetrahedral symmetry. Indeed, as it is

* Presented at the XXV Nuclear Physics Workshop “Structure and Dynamics of Atomic Nuclei”, Kazimierz Dolny, Poland, September 25–30, 2018.

well-known from group theory, an appropriate realisation of the tetrahedral symmetry for the systems of Fermions is the so-called double tetrahedral-group T_d^D . The latter has two 2-dimensional and one 4-dimensional irreducible representations. As a consequence, and in contrast to the case of the ‘usual’ deformations studied so far, the nucleonic spectra of tetrahedral-deformed nuclei are composed of three families of levels, those belonging to the 4-dimensional representation carrying up to 4 nucleons per level. These properties gave rise to the introduction, in the cited reference, of a new labelling system of the corresponding single-particle levels as an alternative to the traditional Nilsson labelling.

The presence of tetrahedral symmetry minima in many nuclei throughout the Periodic Table has been predicted in Ref. [2] with tetrahedral magic numbers $Z^t, N^t = 32, 40, 56, 64, 70, 90, 112, 136$. The possible presence of the tetrahedral symmetry minima in the $Z = N$ nuclei in the mass $A \sim 70$ region has been suggested with the help of the Skyrme HF method in Ref. [3].

As the next step of the evolution, it has been predicted in Ref. [4] that the tetrahedral deformations should be accompanied by the octahedral one, the new symmetry corresponding to the point-group O_h , in several nuclei of the rare-earth region. This prediction has been confirmed using the experimental data *versus* theory modelling in the recent Ref. [5], in which the results obtained with the spin-parity and particle-number projected HFB methods together with the group-theory methods have been employed.

In the present article, we address the question of *how universal the mechanism of the simultaneous presence of the two deformations is*. In particular, it has been pointed out in Refs. [4, 5] that in the rare-earth nuclei, one should expect the coexistence of these two deformations, whereas in the recent Ref. [6], it has been predicted that the same should be expected for at least some actinide nuclei. In this article, we will focus on the lighter nuclei of (and around) zirconium, in which the above property is predicted by us *not to apply*. The issue attracts certain specific interests in terms of interpreting the observed nuclear shape symmetries and symmetries more generally, as the result of the spontaneous symmetry breaking, *e.g.* octahedral by tetrahedral one. Indeed, on the one hand, the tetrahedral symmetry group is the sub-group of the octahedral one, whereas on the other, the signs of the simultaneous presence of the two may be seen as a manifestation of the spontaneous breaking of the symmetry generated by a given group by one of its subgroups.

2. Evolution of concepts about identification criteria for nuclear tetrahedral symmetry

Let us briefly remind the reader about evolution of the ideas concerning criteria of identification of the tetrahedral symmetry in atomic nuclei.

2.1. Early ideas based on collective model and the zero-point motion

To begin with, it will be instructive to consider a typical structure of the potential energy surface in a doubly-magic tetrahedral symmetry nucleus. Figure 1 presents the case of the tetrahedral doubly-magic $^{154}_{64}\text{Gd}_{90}$ as an example. As one can see from the figure, in addition to the ‘usual’ competition between the prolate and oblate axially symmetric minima, one finds the characteristic pair of low-lying symmetric tetrahedral-symmetry minima at $\alpha_{32} \approx \pm 0.13$ and $\alpha_{20} = 0$.

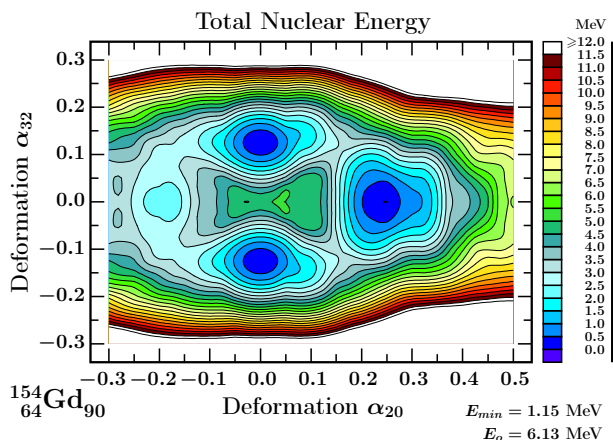


Fig. 1. Shape competition: Quadrupole minimum at $\alpha_{20} \approx 0.22$, and tetrahedral one with symmetric minima at $\alpha_{32} \approx \pm 0.13$; Woods–Saxon mean field, Ref. [7].

Since the orientation of quantum tetrahedral-deformed objects can be defined (in contrast to the objects of spherical symmetry), they may generate rotational bands with the rotational energies satisfying $E_I \propto I(I + 1)$. One can demonstrate using simple geometrical arguments that the dipole and quadrupole moments of the tetrahedral-symmetric nuclei vanish. It follows that the quadrupole transitions, which dominate the de-excitations patterns of the rotational bands vanish — as well as the dipole transitions. Thus, one could expect an existence of the excited rotational states with vanishing E2 transitions, thus possibly manifesting a sequence of isomeric states with $E_I \propto I(I + 1)$ spacing.

Following the elementary notions of collective nuclear oscillations, one needs to consider the zero-point motion of at least two vibrational modes: The one, also called ‘tri-axial octupole’ or α_{32} -tetrahedral oscillation and the quadrupole oscillation in the direction of α_{20} , which dynamically¹ breaks tetrahedral symmetry and induces non-vanishing quadrupole moments.

Moreover, increasing angular momentum of rotation which contributes to the partial individual angular momentum alignments due to Coriolis effects, distinguishes a direction in space and contributes in addition to the zero-point motion to the tetrahedral symmetry breaking. Thus, it has been suggested in a number of publications that due to the dynamical presence of the quadrupole oscillations and the nucleonic alignment, the $B(E2)$ transitions are never strictly zero. According to such a picture, one would expect that at relatively high angular momenta, the tetrahedral configurations induce some E2 transitions due to symmetry breaking especially since the transition probabilities are proportional to $(\Delta E_\gamma^{E2})^5$. Such transitions, however, cease existing at the bottoms of the bands giving rise to the presence of the $E_I \propto I(I+1)$ energies not connected via E2 transitions anymore.

It turns out that experimental data on several nuclei satisfy these criteria, as *e.g.* the results on ^{154}Gd illustrated in Fig. 2, but as long as the $B(E2)$ values are not measured, the above interpretation remains a hypothesis. The specifically designed measurements were performed using ultra-high resolution γ -ray spectroscopy on the neighbouring ^{156}Gd nucleus, in which an analogous band structure exists, Ref. [9]. Results indicate that the quadrupole moment of the corresponding negative parity band is very close to the quadrupole moment of the ground state. Today, it is believed that the E2 transitions, whose probabilities are proportional to $(\Delta E_\gamma^{E2})^5$, loose in competition with the E1 transitions to the ground-state band when the spin decreases, given the fact that ΔE_γ^{E2} decrease quickly, whereas ΔE_γ^{E1} are of the order of 1 MeV and sometimes even increase with decreasing spin, *cf.* Fig. 2. We may plausibly expect that similar conclusions apply to the neighbouring nuclei in this region.

Thus, the discussed negative-parity bands, which were originally interpreted as possibly carrying signs of tetrahedral symmetry, should rather be interpreted as axially-symmetric pear-shape octupole-vibration bands. In the meantime, a more rigorous interpretation has been developed in terms of the spin-, and particle-number projected Hartree–Fock–Bogolyubov approach and the group theory, by the Fukuoka–Strasbourg collaboration, Refs. [10, 11] and [6]. The main results are summarised below.

¹ Let us note that the concept of the zero-point motion inherent to the collective model proposed originally by A. Bohr strictly speaking invalidates the concept of any geometrical symmetry. Indeed, accepting the presence of the zero-point motion for at least/only quadrupole ($\alpha_{\lambda=2,\mu=0,2}$) and octupole ($\alpha_{\lambda=3,\mu=0,\pm 1,\pm 2,\pm 3}$) modes is not compatible with any static geometrical symmetry of the nuclear surface.

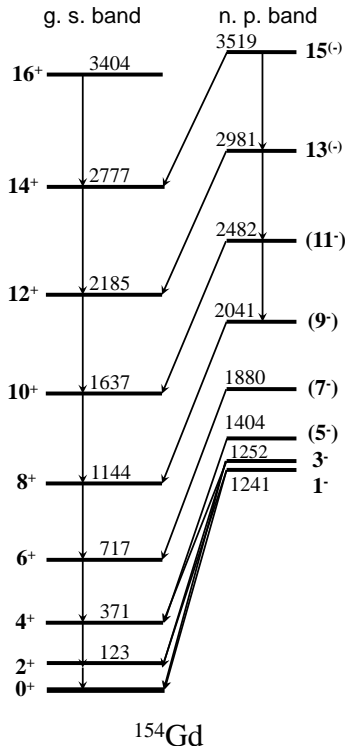


Fig. 2. Experimental results for the two rotational bands in ^{154}Gd ; the data are from Ref. [8].

2.2. Recent evolution: ideas based on the group theory considerations

Let us consider double point-group T_d^D as the symmetry group of a mean-field Hamiltonian, H_{mf} . We will also introduce an auxiliary tetrahedral-symmetric quantum rotor Hamiltonian, H_{rot} . It will be used as a discussion reference for the case of rotating even-even tetrahedral-symmetric nuclei and for this reason, H_{rot} will be assumed invariant under the T_d -group.

We will be interested in the properties of the quantum rotor spectra resulting from the quantum-rotor Hamiltonian symmetry-properties. These can be conveniently described with the help of the irreducible representations of the symmetry group in question. Tetrahedral T_d -group has 5 irreducible representations, here denoted A_1 , A_2 , E , F_1 and F_2 . Whereas a more complete discussion of the spectral properties of various bands generated by the quantum rotor in question can be found in Ref. [6] and references therein, here and in what follows, we will limit our discussion to the unique, ‘tetrahedral ground-state band’ having as the band head the $I^\pi = 0^+$ state.

Using the theory of group representations and the tables of group characters, one may demonstrate that the collective band built on the $I^\pi = 0^+$ tetrahedral ground-state is composed of the A_1 -representation states with the following spin-parity combination, *cf. e.g.* Refs. [10–12]:

$$A_1 : \quad 0^+, 3^-, 4^+, \underbrace{(6^+, 6^-)}_{\text{doublet}}, 7^-, 8^+, \underbrace{(9^+, 9^-)}_{\text{doublet}}, \underbrace{(10^+, 10^-)}_{\text{doublet}}, 11^-, \underbrace{2 \times 12^+, 12^-}_{\text{triplet}}, \dots$$

Forming a common parabola

(1)

The presence of the characteristic parity doublets and a complete lack of the $I = 1$ and 2 states deserves noticing.

It has been demonstrated in Refs. [10, 11] by explicit microscopic calculations using the spin-parity and particle number projected Hartree–Fock–Bogolyubov cranking approach with the Gogny interactions, that the E_I -vs.- I rotational sequences predicted by the tetrahedral symmetric field manifest the above quantum-rotor properties to a remarkable approximation, whose degree increases with the tetrahedral deformation increasing.

It then follows that in order to be able to advance in the discussion of the coexistence between the tetrahedral and octahedral symmetries in nuclei and in particular to propose the experimentally applicable identification criteria, it will be of particular importance to establish the similar features for the rotor Hamiltonians with the octahedral symmetry as well. One may apply the same methods of the group representation theory to conclude that in the case of the octahedral symmetry, the lowest energy part of the spectrum of the rotor takes the form of two branches, one with positive

$$A_{1g} : \quad 0^+, 4^+, 6^+, 8^+, 9^+, 10^+, \underbrace{(12^+, 12^+)}_{\text{doublet}} \dots, \quad I^\pi = I^+$$

Forming a common parabola

(2)

and one with the negative parity

$$A_{2u} : \quad \underbrace{3^-, 6^-, 7^-, 9^-, 10^-, 11^-, 12^-}_{\text{Forming another (common) parabola}}, \dots, \quad I^\pi = I^-,$$
(3)

where the role of the A_1 representation in the previous case is played by A_{1g} and A_{2u} in the present case. The bands defined in Eqs. (1)–(3) are illustrated qualitatively in Fig. 3.

The discussed symmetry properties have been used in Ref. [5] to identify the combination of octahedral and tetrahedral symmetries using existing experimental data on ^{152}Sm nucleus.

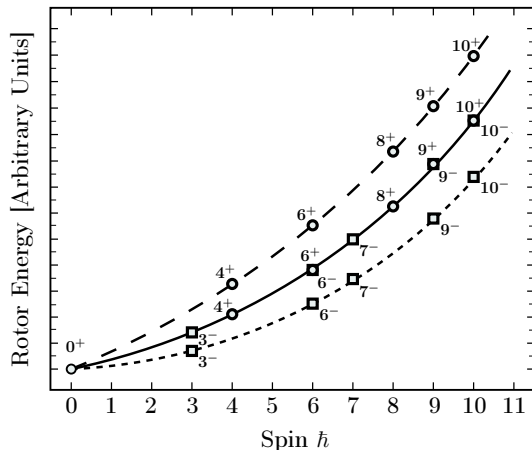


Fig. 3. Schematic: Tetrahedral symmetry band, full line, composed simultaneously of positive and negative parity states, some of them (6^\pm , 9^\pm , 10^\pm) degenerate, *cf.* Eq. (1). Dashed lines illustrate the positive and negative parity octahedral band-partners, *cf.* Eqs. (2)–(3). According to the discussed criteria, the pure tetrahedral symmetry case should result in one band with both parity states forming approximately a common parabola, whereas dominating octahedral symmetry might lead to two close-lying but well-separated bands of the opposite parities as schematically illustrated.

3. Possible T_d -vs.- O_h coexistence: present or missing

As announced in the preceding sections, we wish to provide more details about the possible scenarios as compared to the case identified in ^{152}Sm in Ref. [5]. We begin with the situation characteristic for the rare-earth nuclei.

3.1. Example of T_d -vs.- O_h coexistence: rare-earth nuclei

Figure 4 illustrates the effect of the coexistence between the two symmetries in the case of one of the double-magic tetrahedral nuclei from the rare-earth range: ^{154}Gd , direct neighbour of ^{152}Sm mentioned earlier. The potential energy projection shown here should be directly compared with the one in Fig. 1. As one can see from the figure, tetrahedral and octahedral deformations co-exist, the result deduced from the presence of the two symmetric minima corresponding to $\alpha_{32} \approx \pm 0.12$ showing at the same time that the tetrahedral-symmetry minimum is lowered by over 1 MeV when the minimisation over o_4 is allowed. Moreover, a pure octahedral symmetry minimum ($\alpha_{32} = 0$ and $o_4 \approx 0.06$) is predicted to coexist in this case.

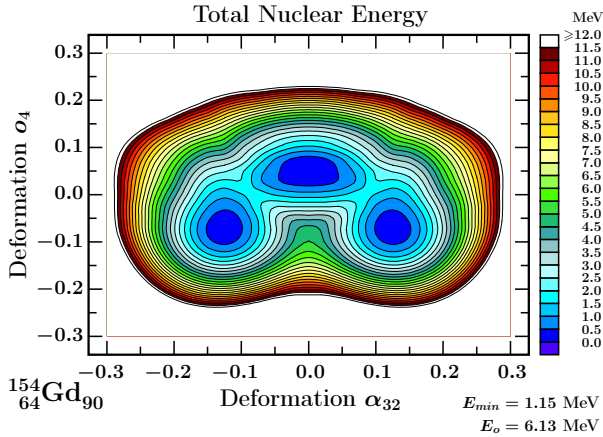


Fig. 4. Total energy calculations analogous to those shown in Fig. 1 but for the octahedral ($o_4 \leftrightarrow \{\alpha_{40}, \pm\sqrt{5/14}\alpha_{4,\pm 4}\}$) and tetrahedral (α_{32}) deformation projection; for the exact definition of the octahedral deformation *cf.* Ref. [13]. These results suggest two high-rank symmetry mechanisms: Pure octahedral symmetry configuration corresponding to $\alpha_{32} \approx 0$ at $o_4 \approx 0.06$, and the double minimum of the combined tetrahedral, $\alpha_{32} \approx \pm 0.12$, and octahedral, $o_4 \approx -0.08$ deformations.

3.2. Counter example: pure tetrahedral symmetry in zirconium region

Figure 5 illustrates an appropriate potential energy surface for ^{96}Zr . Results show a pure tetrahedral-deformed ground-state minimum in this nucleus. Let us notice that a deformed nucleus at the $I^\pi = 0^+$ (here:

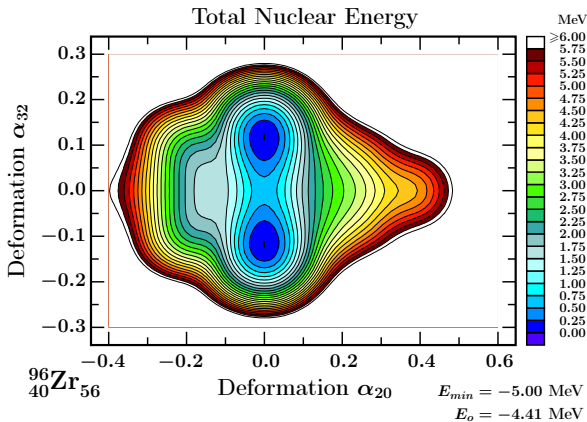


Fig. 5. Total nuclear energy surface for ^{96}Zr projected onto the $(\alpha_{20}, \alpha_{32})$ deformation plane showing two symmetric tetrahedral symmetry minima at $\alpha_{32} \approx \pm 0.12$. The importance of this indication is enforced by the results presented in Table I and showing a very high value of the $B(E3)$ value associated with the first $I^\pi = 3^-$ excitation in this nucleus.

ground) state appears in any laboratory frame as spherical. The same is approximately true for any particle-hole excited configurations coupled to the $I^\pi = 0^+$ core of $(A - 2)$ nucleons. It would be extremely important to attempt identifying in this nucleus the predicted tetrahedral symmetry rotational bands using the mass spectrometry methods as suggested in Ref. [6]. Furthermore, Fig. 6 shows that in the case of ^{96}Zr deformation o_4 has no major effect on the absolute minimum of the total energy, therefore reinforcing the argument of a pure tetrahedral symmetry configuration for this nucleus, in contrast to the previous case of ^{154}Gd .

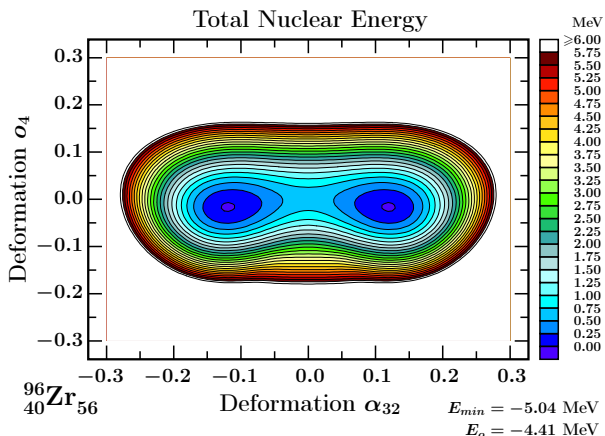


Fig. 6. Illustration similar to the one in Fig. 4 showing two symmetric tetrahedral symmetry minima at $o_4 \approx 0$ indicating no coexistence between tetrahedral and octahedral degrees of freedom in contrast to the previous case; these results predict a pure tetrahedral symmetry configuration.

Experimental data in Table I show particularly high values of the $B(E3)$ reduced transition probabilities in nuclei in the vicinity of the doubly magic tetrahedral nucleus ^{96}Zr thus providing support to the predictions of a strong

TABLE I

Experimental values of the reduced transition probabilities $B(E3)$ in Weisskopf units for the first $I^\pi = 3^-$ excitation; from NNDC <http://www.nndc.bnl.gov>

Nucleus: Z vs. N	52	54	56	58	60
^{64}Pd	—	—	—	—	29 ± 10
^{44}Ru	—	—	14 ± 3	—	—
^{42}Mo	—	—	31 ± 4	35 ± 3	—
^{40}Zr	18.3 ± 11	—	57 ± 4	—	—
^{38}Sr	—	18.3 ± 11	—	—	—

octupole effects in this nuclear range. Similar results are predicted to hold for another doubly-magic tetrahedral nucleus, $^{104}_{40}\text{Zr}_{64}$. Results in Fig. 7 show that the tetrahedral minimum corresponds again to the ground state for the nucleus, since the absolute minima appear at $a_{32} \sim 0.16$, $a_{20} \sim 0.0$ and $o_4 \sim 0.0$. However, at the same time, the super deformed minimum at $a_{20}^{\text{th}} \sim 0.38$ is also predicted together with the oblate shape minimum at $a_{20}^{\text{th}} \sim -0.20$. These predictions are comparable to the experimental quadrupole deformations of the neighbouring nuclei ^{102}Zr and ^{106}Mo , which are $a_{20}^{\text{exp}} = 0.427 \pm 0.044$ and $a_{20}^{\text{exp}} = 0.354 \pm 0.009$, respectively, Ref. [14].

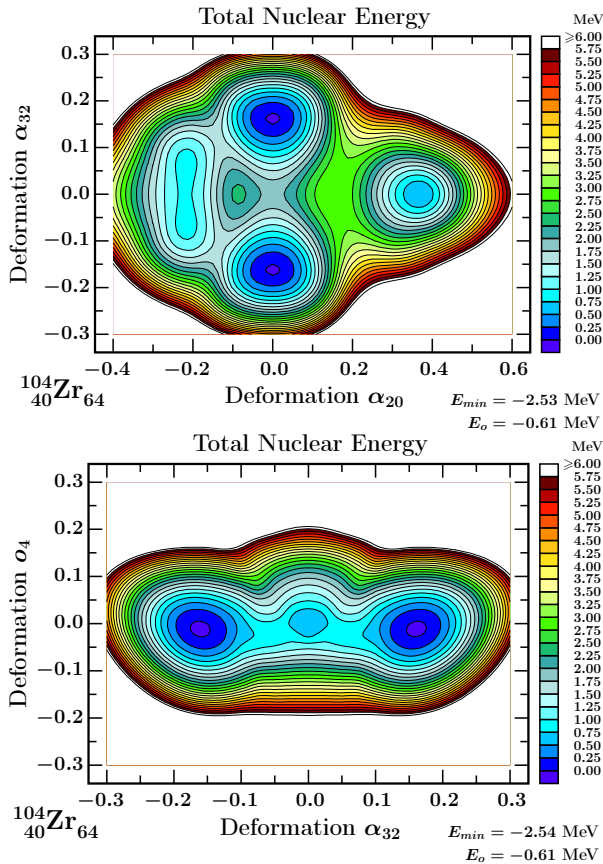


Fig. 7. Top: Total nuclear energy surface for ^{104}Zr projected onto the $(\alpha_{32}, \alpha_{20})$ deformation plane. Bottom: Total nuclear energy projected onto the (o_4, α_{32}) deformation plane. In this case, the pure tetrahedral deformed minimum appears to be again the ground state but the strongly deformed ($\alpha_{20} \sim 0.38$) and oblate ($\alpha_{20} \sim -0.2$) shapes are also predicted.

4. Summary and conclusions

We discussed the theory predictions related to the possible competition between the exotic tetrahedral and octahedral nuclei and the corresponding criteria of the experimental identification. According to our predictions, in the zirconium nuclei, tetrahedral deformations appear not to be accompanied by the octahedral ones, in contrast to the rare-earth and actinide nuclei. Experimental manifestation of this prediction is expected to take the form of a single parabolic branch composed of states $I^\pi = 0^+, 3^-, 4^+, 6^\pm, 6^-, 8^+, 9^\pm, \dots$, and can be today studied using mass spectrometry methods.

This work was partially supported by the National Science Centre, Poland (NCN) under contract No. 2016/21/B/ST2/01227, the Polish–French COPIN-IN2P3 collaboration agreement under project numbers 04-113 and 05-119, and by the Polish–French collaboration project LEA-COPIGAL.

REFERENCES

- [1] X. Li, J. Dudek, *Phys. Rev. C* **49**, 1246 (1994).
- [2] J. Dudek, A. Gózdź, N. Schunck, M. Miśkiewicz, *Phys. Rev. Lett.* **88**, 252502 (2002).
- [3] S. Takami, K. Yabana, M. Matsuo, *Phys. Lett. B* **431**, 242 (1998).
- [4] J. Dudek *et al.*, *Phys. Rev. Lett.* **97**, 072501 (2006).
- [5] J. Dudek *et al.*, *Phys. Rev. C* **97**, 021302 (2018).
- [6] J. Dudek *et al.*, *Acta Phys. Pol. B Proc. Suppl.* **12**, 569 (2019), this issue.
- [7] The *Universal Woods–Saxon Hamiltonian* and associated, so-called ‘universal parametrization’ has been developed in a series of articles: J. Dudek, T. Werner, *J. Phys. G: Nucl. Phys.* **4**, 1543 (1978); J. Dudek *et al.*, *J. Phys. G: Nucl. Phys.* **5**, 1359 (1979); J. Dudek, W. Nazarewicz, T. Werner, *Nucl. Phys. A* **341**, 253 (1980); J. Dudek, Z. Szymański, T. Werner, *Phys. Rev. C* **23**, 920 (1981); and has been summarized in: S. Ćwiok *et al.*, *Comput. Phys. Commun.* **46**, 379 (1987). This approach is being used without modifications by many authors also today.
- [8] C.W. Reich, *Nucl. Data Sheets* **110**, 2257 (2009).
- [9] M. Jentschel *et al.*, *Phys. Rev. Lett.* **104**, 222502 (2010).
- [10] S. Tagami, Y.R. Shimizu, J. Dudek, *Phys. Rev. C* **87**, 054306 (2013).
- [11] S. Tagami, Y.R. Shimizu, J. Dudek, *J. Phys. G: Nucl. Part. Phys.* **42**, 015106 (2015).

- [12] M. Hamermesh, *Group Theory and Its Application to Physical Problems*, Dover Publications, Inc., New York 1962.
- [13] J. Dudek *et al.*, *Int. J. Mod. Phys. E* **16**, 516 (2007).
- [14] S. Raman, C.W. Nestor, Jr., P. Tikkanen, *At. Data Nucl. Data Tables* **78**, 1 (2001).